Downloaded from www.sjweh.fi on November 18, 2018

Supplement

Scand J Work Environ Health 2004;30(2):63-72

A sectional aerosol model for submicron particles in indoor air

by Asmi AJ, Pirjola LH, Kulmala M

Affiliation: University of Helsinki, Department of Physical Sciences, PO Box 64, University of Helsinki, Helsinki, Finland.

The following articles refer to this text: 2004;30 suppl 2:1-98; 2004;30 suppl 2:1-98

Key terms: aerosol model; indoor aerosols; indoor air; indoor-to--outdoor ratio; modeling; submicron particle

This article in PubMed: www.ncbi.nlm.nih.gov/pubmed/15487687

This work is licensed under a Creative Commons Attribution 4.0 International License.

Print ISSN: 0355-3140 Electronic ISSN: 1795-990X Copyright (c) Scandinavian Journal of Work, Environment & Health

Original article

Scand J Work Environ Health 2004;30 suppl 2:63–72

A sectional aerosol model for submicron particles in indoor air

by Ari J Asmi, MSc,[1, 2] Liisa H Pirjola, PhD,[1] Markku Kulmala, PhD[1]

Asmi AJ, Pirjola LH, Kulmala M. A sectional aerosol model for submicron particles in indoor air. *Scand J Work Environ Health* 2004;30 suppl 2:63–72.

Objectives This study attempted to simulate indoor concentrations and the indoor-to-outdoor (I:O) number concentration ratios of aerosol particles in the submicron size range.

Methods The developed model used size-segregated outdoor number concentrations of particles as inputs and produced the indoor aerosol size spectrum. It covered all the major dynamic processes associated with the indoor aerosol concentration: transport and filtration in the air exchange system, deposition, coagulation, nucleation, condensation, and indoor sources. The model results were compared with measured particle concentrations. Numerous sensitivity analyses were also made for testing the effect of different dynamic processes on the model results. No indoor particle sources were considered in the sensitivity simulations.

Results Changes in the air exchange rate had the strongest effect on the simulated I:O ratios of particle number concentrations. Filtration in the air exchange system also had a large effect on the indoor concentrations. Deposition did not significantly change the particle number concentrations within a realistic range of turbulence intensity indoors and the temperature differences between the ambient air and surfaces. Coagulation affected only the smallest particle size ranges. Condensation and nucleation had potentially large effects on the particle size spectrum.

Conclusions The model reproduced the measured I:O ratios of fine and ultrafine particle concentrations with reasonable accuracy. The model can be a valuable tool with which to estimate the I:O ratios for human exposure assessment.

Key terms indoor aerosols, indoor-to-outdoor ratios, modeling.

The acute and chronic health effects of fine (mean aerodynamic diameter <2.5 μm) and ultrafine (mean aerodynamic diameter <0.1 μm) particles in ambient air have recently raised considerable interest (1). The associations of adverse health outcomes with outdoor mass concentrations of aerosol particles have traditionally been the main focus of research. Usually, one centrally located outdoor measurement site has been selected to give a representative exposure estimate for a population living in a large urban area. This approach has several drawbacks. First, people spend most of their time indoors in developed countries, and, therefore, indoor air quality has a considerable impact on the population exposure to air pollution (2). Second, both indoor and outdoor environments have natural and anthropogenic sources of ultrafine particles (3, 4). Third, if the relationships between indoor and outdoor pollution levels are not known, the actual exposures of population groups from outdoor sources cannot be assessed. Studies using personal monitoring of particulate exposures have attempted to circumvent some of the listed drawbacks (5).

The indoor-to-outdoor ratio (I:O) of different kinds of aerosols has been studied earlier. Most of these studies focused on the differences in average mass concentration. It is only recently that spatially and temporally more-detailed information has been obtained for different particle size ranges. In the absence of common indoor sources (eg, tobacco smoke), the I:O ratios of fine particulate mass concentrations have been slightly below 1.0 for both office and home environments (6). In a recent Finnish study (7), the I:O ratios of particle number concentrations in the size range of 0.007–0.5 μm in one office building were strongly dependent on the particle size and the ventilation system settings. Indoor ultrafine particle concentrations were normally much smaller than the outdoor ones, even though they followed the same temporal pattern. In a study in a large office building in the United States (8), similar results

1 University of Helsinki, Department of Physical Sciences, Helsinki, Finland.
2 Ford Research Centre Aachen, Aachen, Germany.

Reprint requests to: Professor Markku Kulmala, University of Helsinki, Department of Physical Sciences, PO Box 64, University of Helsinki, Helsinki, Finland. [E-mail: markku.kulmala@helsinki.fi]

were found with I:O ratios of particle number concentrations between 0.15 and 0.28. Both studies observed a minimum I:O ratio between particle diameters of 0.3 and 0.7 μm, this result probably reflecting a combined effect of filtration with fibrous filters and deposition of the smaller and larger particles.

Simulation models have been used to estimate the indoor concentrations of aerosol particles. Most of them are based on a simple mass balance approach that leads to a general equation for time evolution of the average mass concentration of indoor air particles C (g/m^3) (9):

$$\frac{dC}{dt} = f(pO_m(t) - C) - C\lambda + S(t), \qquad \text{equation 1}$$

where f (s^{-1}) is the air exchange rate, p is the penetration coefficient, $O_m(t)$ (g/m^3) is the mass concentration of outdoor air particles, λ (s^{-1}) is the deposition parameter, and $S(t)$ [g/(m^3·s)] represents the sum of all other sources and sinks indoors. This equation is generally applicable for all indoor pollutants and has been extensively used in the literature (10). Improved versions of this model have been constructed by using the mass balance of indoor surfaces as an integral part of the calculation (11). Lately, the basic model has also been modified to simulate, for example, fast chemical processes indoors (12) and the differences in air quality between corridors and offices (13).

The mass balance models usually depend on several experimentally defined parameters, and they are often unable to predict complicated aerosol phenomena, mainly due to the strong influence of particle size on the filtration and deposition of particles. If real-life particle size distributions differ from the ones used to estimate size-dependent parameters, the model results may be erroneous. For this reason, some authors have used approaches involving particle-size dependent models, for example (14).

Model complexity is a controversial issue in the modeling of indoor aerosols. Models that are too complicated need a lot of information about the modeled environment, they are sensitive to measurement errors, and their results cannot be generalized. Therefore a single-compartment indoor model that takes into account the different particle sizes seems to be a good compromise (15).

The principal objective of our study was to describe different dynamic effects affecting the concentration and size distribution of submicron particles in indoor air. Moreover, we also compared the simulated and measured I:O ratios and analyzed indoor aerosol data with the model. In the model development, the following basic requirements needed to be fulfilled: (i) the inclusion of all relevant aerosol processes affecting indoor particle size distributions, (ii) the ability to use measured size distributions as inputs, (iii) easy comparison of modeled data with direct measurements, (iv) the ability to simulate most controlled (ie, ventilated) indoor microenvironments accurately and uncontrolled (ie, unventilated) microenvironments sufficiently, and (v) the possibility for generalizing the results.

Material and methods

Model description

The present indoor aerosol model takes a sectional approach, which has been commonly used in both indoor and outdoor studies (15, 16). The sectional method gives a reasonably accurate description of the particle size distribution if the number of sections is large enough. It has an additional benefit in that it does not require the size distribution to follow any known modal structure as the "modal" methods do (17).

Our sectional indoor aerosol model is based on the aerosol dynamics model AEROFOR (16). Numerical diffusion was controlled using a relatively large number of sections—in most simulations, 62 logarithmically evenly spaced sections between 0.001 and 1 μm of particle dry diameter. A sensitivity analysis showed that the use of more than 62 particle size sections did not change the modeling results in our case studies.

The particles were assumed to consist of water and some general condensable vapor (GCV) that was defined as species with (i) a low saturation vapor pressure in ambient conditions, (ii) common presence in indoor environments, (iii) either primary or secondary (ie, via chemical reactions) sources indoors, and (iv) high solubility in water. In several parts of our model, the GCV was represented by sulfuric acid. By assuming that the aerosol particles were spherical, we could estimate the number of GCV moles in a single aerosol particle in the first section from the following equation:

$$n_i = \frac{1}{6}\pi d_{p\,dry}^3 \frac{\rho_{GCV}}{M_{GCV}}, \qquad \text{equation 2}$$

where $d_{p\,dry}$ (m) was the dry diameter of the aerosol particles, M_{GCV} (g/mol) was the molar mass of the GCV, and ρ_{GCV} (g/m^3) was the density of the GCV. The particles were assumed to be in equilibrium with the water vapor indoors (16).

The dry size distribution of the aerosol particles was divided into i_{max} size sections, and the aerosol dynamics were considered to be similar for all particles in one section (16, 18). The time derivative of the number concentration N_i (m^{-3}) in size section i could then be presented as equation 3:

$$\frac{dN_i(t)}{dt} = \sum_{l=1}^{l_{\max}} J_i^l, \qquad \text{equation 3}$$

where J^l_i (m^{-3}/s) was the rate of process l to the number concentration in the section and l_{max} was the number of dynamic processes included in the calculation. The dynamic processes that we considered in this sectional model are described in the following text.

Ventilation and filtration. The most important factor affecting the relationship between outdoor and indoor aerosol concentrations was the ventilation system. Modern office buildings have usually been installed with mechanical ventilation systems. The air exchange rate (s^{-1}) in a single room can be expressed as equation 4:

$$f = \frac{F}{V_{room}}, \qquad \text{equation 4}$$

where F (m^3/s) is the air volume flow rate through the ventilation system to and from the room and V_{room} is the free air volume of the room (m^3) (19). The penetration of aerosol particles in size section i through fibrous filters in a mechanical ventilation system was defined as follows:

$$p_i = \frac{N_i}{O_i}, \qquad \text{equation 5}$$

where p_i is the penetration coefficient and N_i and O_i are the indoor and outdoor number concentrations (m^{-3}) in size section i (20).

We used a general filtration model for clean filters with the assumption that filtration by each fiber was an independent process. Thus the filtration efficiency for each particle size section could be presented as follows:

$$E_i = \exp\left(\frac{-4\alpha_f E_{\Sigma,i}(\alpha_f, v_f, d_f)}{\pi d_f} x_s\right), \qquad \text{equation 6}$$

where α_f is the porosity parameter, d_f (m) is the representative fiber diameter, $E_{\Sigma,i}$ is the single-fiber filtration efficiency, v_f (m/s) is the average velocity of air in the filter, and x_s (m) is the filter thickness (20). Interception and diffusion were considered to be the most important filtration processes.

In our model, the overall effect of building ventilation and filtration on the indoor number concentration J^v_i (m^{-3}/s) in size section i was as follows:

$$J_i^v = f(O_i(t)p_i - N_i(t)). \qquad \text{equation 7}$$

Deposition. Particle flux density to surfaces due to deposition I_D [m^{-3}(m/s)] was defined as

$$I_D(d_p) = v_d(d_p)N_\infty(d_p), \qquad \text{equation 8}$$

where v_d (m/s) is the deposition velocity and N_∞ (m^{-3}) is the number concentration far from the surface.

The deposition velocity to smooth, horizontal, and upward-facing surfaces, $v_{d\,hu}$ (m/s), was

$$v_{d\,hu} = \frac{v_g}{1 - \exp(-v_g / v_{dv})}, \qquad \text{equation 9}$$

where v_{dv} (m/s) is the deposition velocity to vertical surfaces and v_g (m/s) is the sedimentation velocity (21). The corresponding equation for horizontal downward-facing surfaces, $v_{d\,hd}$ (m/s), was

$$v_{d\,hd} = \frac{v_g}{\exp(v_g / v_{dv}) - 1}, \qquad \text{equation 10}$$

which also included the deposition velocity to vertical surfaces as a controlling variable (21).

Turbulent diffusivity, D_t (m^2/s), dominated the particle transport, and it was accounted as

$$D_t = K_e y^m, \qquad \text{equation 11}$$

where K_e (s^{-1}) is the turbulence parameter, y is the perpendicular distance from surface m, and m is a free parameter (22). In our simulations, a value of 2 was used for m due to dimensional constraints. In this case, v_{dv} (m/s) could be approximated by the following equation:

$$v_{dv} = \frac{2}{\pi}(D_b K_e)^{1/2}, \qquad \text{equation 12}$$

where D_b (m^2/s) is the Brownian diffusivity of the particles (21).

The thermophoretic effect in deposition could be included in our model. The combined deposition velocity, v_d (m/s), including both thermophoretic and diffusional effects, was

$$v_d = v_d^{dif} - k_t \frac{T_s - T}{T} \nu_{air} \frac{(K_e/\alpha)^{1/2}}{\tan^{-1}\left[\delta_{bl}(K_e/\alpha)^{1/2}\right]}, \qquad \text{equation 13}$$

where v_d^{dif} (m/s) is the deposition velocity from equations 9, 10, and 12 to the surface, k_t is the thermophoretic coefficient, T_s (K) is the temperature at the surface , ν_{air} (m^2/s) is the kinetic viscosity of air, α (m^2/s) is the thermal diffusivity of air, and δ_{bl} (m) is the fluid boundary-layer

thickness near the surface (23). The boundary-layer thickness was difficult to obtain directly and therefore had to be approximated from semiempirical equations (23).

Recently, Lai & Nazaroff (24) developed another formulation of deposition velocity to vertical surfaces by assuming that turbulent diffusivity could be closely approximated by kinematic viscosity, while using the friction velocity, u^* (m/s), as the key parameter as follows:

$$v^+_{dv} = u^* / I$$

$$I = \int_{r^+}^{30} \left(\frac{\nu_{air}}{D_b + D_t} \right) dy^+, \qquad \text{equation 14}$$

where the dimensionless variables are $v^+_{dv} = v_d / u^*$, $y^+ = yu^*/\nu_{air}$, $r^+ = (d_p/2)(u^*/\nu_{air})$, d_p (m) is the radius of wet aerosol particle, and I is the deposition integral. The upper boundary of the integration was set at an approximate height of the boundary layer near the surface. In our present model, we used the functional fits of Lai & Nazaroff (24) for the values of I.

The overall fluxes to and from surfaces J_i^d (m^{-3}/s) in particle size section i were calculated by adding the deposition velocities and re-emission from all available surfaces as follows:

$$J_i^d = \sum_{k=1}^{m_{surf}} \frac{A_k}{V_{tot}} \left[v_d^k N_i(t) - z_i^k R_i^k(t) B_i^k(t) \right] \qquad \text{equation 15}$$

where $k = 1,..., m_{surf}$, m_{surf} is the number of different surfaces indoors, A_k (m^2) is the area of surface k, z^k_i is the ratio of deposited particles available for re-remission from surface k to the total deposited particles on that surface, R^k_i (s^{-1}) is the re-emission rate of section i particles from surface k, and B^k_i (m^{-2}/s) is the surface accumulation of particles on surface k. The deposition velocities were calculated from equations 9–12 and, as an alternative for the vertical wall deposition, from equation 14. The model took either K_e or u^* as the input parameter.

Coagulation. Coagulation is one of the basic dynamic aerosol processes that describes the effect of particle collisions on the aerosol population. The driving force in the collisions is the relative velocity differences between the particles. The coagulation rate, $J_{j,k}$ (m^{-3}/s), between particle populations of size sections k and j could be defined as follows:

$$J_{j,k} = K_{j,k}(d_{pj}, d_{pk}) N_j N_k, \qquad \text{equation 16}$$

where $K_{j,k}$ is the coagulation coefficient (m^3/s), d_{pj} and d_{pk} are the particle diameters in size sections j and k, and N_j and N_k are the particle number concentrations in size sections j and k, respectively (3).

Only Brownian and gravitational coagulation were considered, although other kinds of coagulation also exist, such as electrostatic and turbulent coagulation (3). Brownian coagulation was usually considered to be the most important coagulation process for fine and ultrafine aerosol particles. The Brownian coagulation coefficient increases rapidly as the size difference between colliding particles increases, and, as such, its effect was the most significant with respect to the smallest particle sizes. Brownian coagulation was calculated according to the Fuchs formulation of the coagulation coefficient (25). We considered gravitational coagulation from different kinds of kinetic coagulation processes. In gravitational coagulation, the driving force is the difference in settling velocity between particles. This kind of coagulation is important if there is a significant number of large particles in the indoor air. We used the basic formulation of gravitational coagulation (3).

Coagulation was assumed to be a linear system of Brownian and gravitational coagulation (ie, both processes were assumed to be independent of each other). Thus the overall coagulation coefficient between size sections j and k, $K_{j,k}$ (m^3/s) could be expressed as follows:

$$K_{j,k} = K^B_{j,k} + K^G_{j,k}, \qquad \text{equation 17}$$

where $K^B_{j,k}$ (m^3/s) is the Brownian coagulation coefficient and $K^G_{j,k}$ (m^3/s) is the gravitational coagulation coefficient. The overall change in the number concentration of size section i particles due to coagulation J^{cg}_i (m^3/s) could then be defined as follows:

$$J_i^{cg} = \sum_{j=1}^{i} \sum_{k=j}^{i} \frac{K_{j,k}}{1+\delta_{j,k}} N_j(t) N_k(t) \cdot \frac{(n_j + n_k) - n_{i-1}}{n_i - n_{i-1}} \delta_{n_j+n_k \in]n_{i-1}, n_i]}$$

$$+ \sum_{j=1}^{i} \sum_{k=j}^{i} \frac{K_{j,k}}{1+\delta_{j,k}} N_j(t) N_k(t) \cdot \frac{n_{i+1} - n_j - n_k}{n_{i+1} - n_i} \delta_{n_j+n_k \in]n_i, n_{i+1}]}$$

$$- N_i(t) \sum_{j=1}^{i_{max}} K_{i,j} N_j, \qquad \text{equation 18}$$

where j and k are dummy indices, n_x is the number of GCV moles in particle size section x, and $\delta_{x,y}$ is the Kroenecker delta function between specific sections x and y (16).

Condensation. Mass transfer from the vapor phase to the particulate phase is also one of the main aerosol processes. To our knowledge, it has not been studied much for fine particles in indoor air.

The condensation flux C_i (molecules m^{-3}/s) among the particles in size section i was defined as follows:

$$C_i = 2\pi\beta_m D_{CGV} d_p V_C, \quad \text{equation 19}$$

where V_C (m^{-3}) is the concentration of GCV far from the particle surface, D_{GCV} (m^2/s) is the binary diffusion coefficient of GCV in air, and β_m is the transition regime correction factor (16).

The molar fraction of the GCV was determined by setting the water activities in the vapor and aerosol phases as equal. The total effect of condensation $J^{cn}{}_i$ (m^{-3}/s) could then be presented as follows:

$$J_i^{cn} = \frac{C_{i-1}}{n_i - n_{i-1}} N_{i-1}(t) V_c(t) - \frac{C_i}{n_{i+1} - n_i} N_i(t) V_c(t), \quad \text{equation 20}$$

where V_c (m^{-3}) is the GCV concentration in the air.

Nucleation. New particles can form directly from the gas phase also indoors. The nucleation scheme in the model used binary nucleation of the water–sulfuric acid system (26). On par with earlier assumptions of the condensable vapor, we assumed that GCV behaves like sulfuric acid in this nucleation parameterization. Nucleation could then be expressed as follows:

$$J_n = I_{nucl}\left(\frac{n^* - n_{i-1}}{n_i - n_{i-1}}\delta_{n^*,]n_{i-1},n_i]} + \frac{n_{i+1} - n^*}{n_{i+1} - n_i}\delta_{n^*,]n_i,n_{i+1}]}\right) \quad \text{equation 21}$$

where I_{nucl} (m^{-3}/s) is the homogeneous nucleation rate of the water–sulfuric acid system and n^* is the number of GCV moles in the critical cluster.

Indoor sources. The influence of indoor sources could be very important with respect to indoor air quality (4). For studies of this effect, the model formulation also included the possibility of having different parameterized size distributions for indoor particulate emissions (27, 28). The source terms could then be integrated over the particle size section limits as follows:

$$J_s = S_i, \quad \text{equation 22}$$

where S_i (m^{-3}/s) is the integrated source effect over size section i.

Effect of surface accumulation and outdoor air

In some cases, it can be necessary to simulate the surface accumulation of airborne particulate pollution. This simulation could be important if the studied indoor microenvironment had much activity, which could cause re-emission from the surfaces or if indoor surfaces are very sensitive. In our present model, we estimated the surface accumulation to surface k, B^k_i (m^{-2}) of aerosol particles in size section i by:

$$\frac{d}{dt}B_i^k(t) = v_d^k N_i(t) - z_i^k R_i^k(t) B_i^k(t), \quad \text{equation 23}$$

which has the same notation as equation 15.

The outdoor concentrations of aerosol particles are needed for the simulations. Usually, they are measured, but, in some cases, it may be important to simulate them from some previously known general concentration profile. We used functional outdoor concentrations of particles in the sensitivity tests of our present model as follows:

$$\frac{d}{dt}O_i(t) = g_i(x_1, x_2, \ldots, t), \quad \text{equation 24}$$

where g_i is the functional form of outdoor concentration change and x_1, x_2 ,... are different variables affecting the outdoor particle concentrations (11).

Solution of differential equations

In principle, differential equation 3 should be coupled with equations 23 and 24, and all of them should be simultaneously calculated. In a typical case, however, outdoor particle concentrations are not dependent on indoor concentrations, and re-emission can be assumed to be small and result in independence of the equations. Thus the equation sets could be integrated separately in the present model: first integrating equation 24 for the outdoor concentration profile over one time period, followed by the main equation 3 for indoor aerosol particle size distribution, and lastly integrating equation 23 for accumulated particles on surfaces. The integrations were done numerically on a normal workstation using the backward differentiation method from library routine D02EJF (29).

Comparisons with measurements

We tested the accuracy of our model by using a previously measured dataset (7). The measurements had been made during the winter of 1999 in a large office building located in central Helsinki. The measured particle sizes covered only the diameter range of 0.007–0.5 μm. Therefore, the modeled size range was reduced to cover the sizes between 0.001 and 0.8 μm (dry size), and the aerosol concentration outside this range was assumed to be negligible. Measurements in the office

building included two almost identical DMPS-systems and the measurements of several inorganic and organic gases and ventilation parameters. Table 1 describes the main parameters used in this simulation.

The main idea of this simulation was to determine how well our model could reproduce the measured I:O ratios if most of the input parameters were estimated. This kind of test simulated the typical situation well when not all of the input parameters were available. The filter efficiencies were estimated using a simplified version of the filter model (20). Only the effects of interception, impaction, and Brownian diffusion on the filter efficiencies were considered. The filter parameters selected for this simulation represented clean EU7-class filters, as assessed on the basis of experimental results (30). The resulting parameter values were used also in other simulations (table 2). As the indoor airflow fields were not measured, the necessary turbulence parameters for the deposition velocity equations could not be directly calculated. Thus the friction velocity u^* was postulated to be a constant value for the whole measurement period. The temperature difference between the air and walls was assumed to be small; therefore, the effect of thermophoresis could be neglected in this simulation. With these choices of initial values and model parameters, a comprehensive modeling of the whole measurement period (slightly over 3 weeks) could be done.

Table 1. Model parameters in relation to previously measured data (7).

Parameter	Data type	Value
Room dimensions	Measured	3.5 · 5.5 · 2.5 m
Total volume	Estimated	48 m^3
Total available surface area	Estimated	83.5 m^2
Air temperature	Measured	Varied
Temperature difference between surfaces and air	Estimated	0 K (0°C)
Friction velocity (for all surfaces, u*)	Estimated	1 cm/s
Air pressure	Measured	Varied
Relative humidity	Measured	Varied
Filter parameters	Simulated (EU7)	See table 2

Table 2. Estimated parameters of filters in the mechanical building ventilation system(20)

Parameter	Value
High efficiency filter (~EU7)	
Porosity	0.05
Filter thickness	1.0 mm
Representative fiber diameter	2.5 µm
Face velocity	0.01 m/s
Low efficiency filter (~EU5)	
Porosity	0.05
Filter thickness	1.0 mm
Representative fiber diameter	7.0 µm
Face velocity	0.01 m/s

Table 3. Base case parameters.

Parameter	Value
Room dimensions	3 × 3 × 3 m
Room temperature	298 K (20°C)
Relative humidity	50%
Total surface area	54 m^2
Temperature difference between surfaces and air	0 K (0°C)
Friction velocity (u^*)	1 cm/s
Turbulence intensity parameter (K_e)	1.0/s
Air exchange rate (f)	3.0/h
Filters in ventilation system	None
Average outdoor number concentration of aerosol particles	5000/cm^3

Base case and sensitivity analysis

Sensitivity simulations were made by using the representative set of parameters described in table 3. The base-case parameters were chosen to represent a typical small office room in a well-ventilated office building. The room was assumed to have few pieces of furniture, and thus the deposition was calculated only for the floor, ceiling, and walls of the room. In the base case, there were no indoor sources of particulate emissions, and the walls were at the same temperature as the ambient indoor air.

We assumed that the outdoor aerosol size distribution could always be presented as three lognormal modes. The modal geometric mean diameters and geometric standard deviations were set at fixed values, and the concentrations were changed as a function of time. The functional form of the concentrations simulated the diurnal pattern observed in Helsinki during typical weekdays (7) as follows: morning rush-hour peak followed by lower values in the afternoon, second peak during the evening rush hour, and slow decrease in concentrations towards the night. Table 4 gives the selected values of the outdoor particle concentrations used in the base-case modeling.

The modeling resulted in a large number of size distributions of indoor aerosol particles. Even these could be directly used in human exposure assessment, but we

Table 4. Estimated modal structure of outdoor particle concentrations in the base case.

Parameter	Nucleation mode	Aitken mode	Accumulation mode
Count mean diameter (µm)	0.020	0.10	0.90
Geometric standard deviation	1.6	2.0	2.0
Maximum modal number concentration (cm^{-3})	12000	7000	100
Geometric mean number concentration (cm^{-3})	3500	1450	50
Minimum modal number concentration (cm^{-3})	1000	500	5

concentrated our analyses on the I:O ratios of aerosol particles. By estimating the overall I:O ratio over the simulated period, we could approximate the typical protection that the building shell provided for the occupants. We called this the building protection factor (BPF) and defined it as follows:

$$BPF(d_p) = \frac{\int_{t0}^{t1} N(d_p)dt}{\int_{t0}^{t1} O(d_p)dt}, \qquad \text{equation 25}$$

where the integrals were calculated over the studied time. As a rough estimate, the indoor particle number size distributions could then be estimated for a simulated building by multiplying the outdoor number size distributions by the size-dependent BPF.

Results

Model comparison with measured data

The measured, as reported by Koponen et al (7), and modeled daytime size-dependent BPF values for the 3.5-week study period in 1999 are shown in figure 1. The modeled BPF values were in relatively good agreement with the measured values, although the model seemed to overestimate the sinks of the smallest particles. This overestimation could have been due to an overestimation of the deposition parameter or some feature of our simplified filtration model.

Effects of dynamic mechanisms on the building protection factor

Air filtration in mechanical ventilation systems of buildings is regarded as the most effective passive method with which to decrease the I:O ratio of atmospheric aerosol particles.

The modeling results for two different filter types are shown in figure 2a, and the results for changing the air exchange rate are presented in figure 2b. The use of a better filter effectively reduced the particle concentrations in indoor air. The reductions in the relative indoor concentrations in all the size classes were comparable with the results from earlier simpler models (11, 31). Additional studies showed, however, that the results were very sensitive to the filter parameters, especially to the filter thickness and representational fiber diameter.

Lowering the air exchange rate reduced the BPF or the average I:O ratio as shown earlier with simpler mass-balance models (11).

Our indoor aerosol model had the following two possible representations of indoor deposition rates: one based on the turbulence intensity parameter K_e (equation 12) and the other on the friction velocity u^* (equation 14). The model results for turbulence intensity, friction velocity, and temperature difference between surfaces and air are shown in figure 3. The changes in the turbulence intensity parameter had a relatively small effect on the BPF for all the particle sizes in the base case that had no filter in the building ventilation system. The changes in friction velocity slightly affected the BPF of the nucleation mode particles, whereas the temperature differences between the ambient room air and surfaces had a small effect mainly on Aitken and accumulation mode particles. The effects of these parameters were qualitatively similar in cases with air filtration.

The effect of coagulation on the indoor particle number concentration was investigated in a series of model runs with different filters and outdoor particle

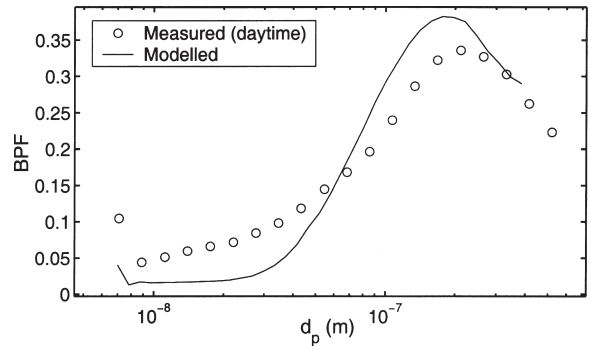

Figure 1. Building protection factor (BPF) as a function of particle diameter (d_p) using both modeled and previously measured (7) daytime particle concentrations in indoor air.

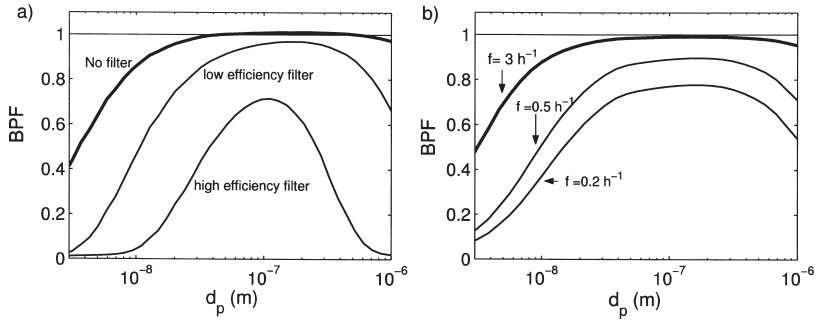

Figure 2. Daily building protection factor (BPF) modeled in the base case with different kinds of filters fitted to the air inlet (see table 2) (a) and as a function of the air exchange rate (f/h) in the office room (b).

number concentrations. Figure 4 shows the results for the Brownian coagulation at different total number concentrations of outdoor air particles and the effect of increasing the GCV in indoor air in the base case.

In a nonfiltered case, the increased outdoor particle concentration strongly decreased the BPF of, especially, the nucleation mode particles due to increased Brownian coagulation indoors.

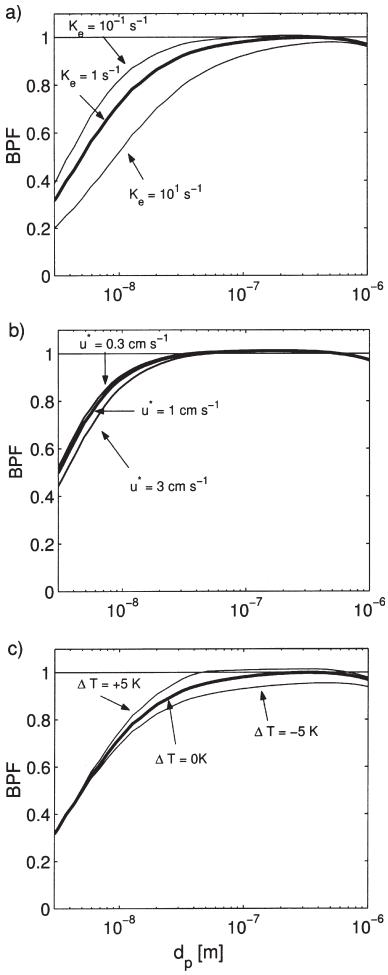

Figure 3. Daily building protection factor (BPF) modeled in the base case as a function of the turbulence parameter K_e (a), friction velocity u*(b), and temperature difference T between room air and surrounding surfaces (when K_e =1/s) (c). Note that the range of parameter change was larger in K_e than in u*.

The addition of even a low efficiency filter practically abolished this effect in simulations, as there was assumed to be no indoor sources of particulate emissions. The highest number concentrations of outdoor air particles represented a situation in which the studied building had a major source of combustion particles (eg, a highway in its immediate vicinity), as otherwise the high coagulation rate would rapidly decrease the outdoor particle number concentration (figure 4a).

The increase in the GCV strongly decreased the BPF of the nucleation mode particles. The condensation of pollutants was simulated for a constantly active emission source on the assumption that the vapor concentration was in a relatively steady state (figure 4b).

Discussion

In this study, we developed a new sectional indoor aerosol model that is more sophisticated than our previous one (11). The model includes all major aerosol dynamic processes and outdoor-to-indoor transport: (i) air exchange and filtration by building ventilation systems, (ii) deposition on horizontal, upward, and downward facing surfaces and vertical surfaces, including thermophoretic and diffusional effects, (iii) Brownian and gravitational coagulation, (iv) condensation of indoor condensable vapors, and (v) indoor emission sources and homogeneous nucleation. The developed model simulates indoor concentrations from measured outdoor data using indoor microenvironmental parameters as inputs. The effect of several dynamic mechanisms on the building protection factor (ie, the daily average I:O ratio) was estimated in the sensitivity analyses of the base case.

We chose a sectional method for representing the size distribution of aerosol particles. This choice somewhat simplified the model structure but required the use of 62 consecutive sections to control the numerical diffusion usually associated with these kinds of models. Another important choice in the model development was the selection of the modeling domain. A direct method to simulate the indoor particle concentration and size distribution would have required heavy computation

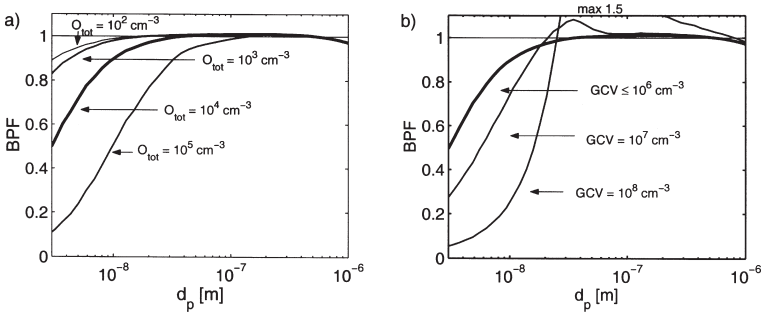

Figure 4. Effect of Brownian coagulation on the building protection factor (BPF) at different total number concentrations of outdoor air particles O_{tot} (a) and the BPF at different general condensable vapor (GCV) levels in indoor air (b).

involving fluid dynamic calculations of flow fields indoors and a subsequent division of calculations of the aerosol dynamics into subgrids. This approach would have had obvious drawbacks related to calculation time and the generalization of the model results for indoor microenvironments from which accurate background data were not available. The need for accurate input data (including measurement errors) would have also reduced the usability of the results. For these reasons, we assumed complete air mixing indoors, and this assumption allowed us to report indoor aerosol distributions and dynamics as average values of the room.

The results showed that both the air exchange rate and the filtration of building ventilation systems should be known accurately. In the case of the air exchange rate, this is not usually a problem, as it is one of the main design parameters in the construction of ventilation systems in buildings. The model was sensitive also to some filter parameters (eg, filter thickness, fiber diameter), for which it can be much harder to obtain accurate values for practical applications of the model. More accurate information on fibrous filters, especially for particles in the ultrafine range, is needed for better model performance. However, the I:O ratios produced by the current filter models were in reasonably good agreement with the measured average values of longer time periods.

Coagulation of particles in the modeled size range can have a substantial effect on indoor number concentrations. In our present model, we included only Brownian and gravitational coagulation. Other kinds of kinetic coagulation happen due to macroscopic velocity differences between the aerosol particles. Accurate information on kinetic coagulation coefficients would be possible if the indoor flow fields were well defined. Such definition is rarely possible even in well-known environments, and significant velocity gradients are high.

We chose the outdoor concentration as the key variable for modeling the effect of coagulation, since the measurements of particle number size distributions are much more common outdoors than indoors. In case of a strong indoor source of particulate emissions (eg, tobacco smoke), the situation could be very different because the indoor number concentrations would be much higher.

The model studies showed that, in the absence of indoor particle sources, the effect of Brownian coagulation could be detected only in the smallest particle sizes if the outdoor number concentration was very high. These kinds of concentrations can be measured if the building ventilation inlet is in close proximity to a relatively strong particle source (eg, highway). The addition of filters to building ventilation systems would decrease the building protection factor of nucleation mode particles and reduce the effect of coagulation indoors. The coagulation results were dependent on the particle size distributions, but realistic changes in the outdoor size distribution did not significantly change the results.

We used two expressions of deposition in our model. Both assumed that indoor air had a turbulent flow pattern, which reduces the usability of the results for houses with low air exchange rates. In the model studies, deposition depended only weakly on the governing turbulence parameters (K_e or u^*). However, here we did assume that deposition happens only on the relatively smooth walls, floor, and ceiling of the indoor microenvironment. With furniture and rough walls, the importance of deposition could increase. The effect of thermophoresis was not significant for the temperature range of ±5 K in the base case. Impaction and electrical currents could have an important effect on deposition, but their main influence would be on particle sizes larger than 1 μm, and the parameters related to them are often hard to define (32).

Condensation could have an important effect on the building protection factor and the I:O ratio of particles. Condensation in our model was approximated from the use of general condensable vapor that behaved like sulfuric acid. This was a good approximation for many potential condensable vapors, but it also represented the upper limit of the condensation rates on the particles, as the vapor pressure in the particle surface was always assumed to be low. Another problem associated with condensation is the multitude of potential condensable vapors indoors. Realistic estimation of the amount of condensation indoors and its effect on any real-life I:O ratio is difficult, as the gas phase concentrations are usually not available. In the case of a strong indoor vapor source, the indoor particles grow rapidly due to condensation, and the I:O ratio of small particles changes significantly. Some assumptions of typical indoor condensable vapors are available, and it has been suggested that some organic species (namely *cis*-pinic acid) could be responsible for some of the detected condensational growth of fine particles indoors (33).

Homogeneous nucleation in indoor environments was included in the model. The used nucleation parameterization was based on a water–sulfuric acid system, which has been extensively studied in atmospheric situations. The gas phase concentrations required for this kind of nucleation are, however, very high, and recently it has been suggested that three-component (ammonia, sulfuric acid, and water) homogeneous nucleation is a more likely nucleation pathway in the atmosphere (34). The addition of this kind of process could be an interesting continuation for our indoor studies, especially since some authors have detected clear particle formation events in indoor microenvironments (7, 33).

In conclusion, our sectional indoor aerosol model can be used for estimating indoor particle number size

distributions using measured outdoor size distributions as input data. The model results improve human exposure assessment for the health risk analysis of particulate air pollution.

Acknowledgments

Our work was funded by the Academy of Finland and the Ministry of Transport and Communications in the Finnish Research Programme on Environmental Health (SYTTY).

References

1. Pekkanen J, Kulmala M. Exposure assessment of ultrafine particles in epidemiologic time-series studies. Scand J Work Environ Health 2004:30 Suppl 2:9–18.
2. Jones A. Indoor air quality and health. Atmos Environ 1999;33:4535–64.
3. Seinfeld JH, Pandis SN. Atmospheric chemistry and physics—from air pollution to climate change. New York (NY): John Wiley & Sons Inc; 1998.
4. Owen MK, Ensor D, Sparks L. Airborne particle sizes and sources found in indoor air. Atmos Environ 1992;26A:2149–62.
5. Koistinen K, Hänninen O, Rotko T, Edwards R, Moschandreas D, Jantunen M. Behavioral and environmental determinants of personal exposures to $PM_{2.5}$ in EXPOLIS—Helsinki, Finland. Atmos Environ 2001;35:2473–81.
6. Wallace L. Indoor particles: a review. J Air Waste Manage Assoc 1996;46:98–126.
7. Koponen IK, Asmi A, Keronen P, Puhto K, Kulmala M. Indoor air measurement campaign in Helsinki, Finland 1999—the effect of outdoor air pollution on indoor air. Atmos Environ 2001;35:1465–77.
8. Fisk W, Faulkner D, Sullivan D, Mendell M. Particle concentrations and sizes with normal and high efficiency air filtration in a sealed air-conditioned building. Aerosol Sci Technol 2000; 32:527–44.
9. Raunemaa T, Kulmala M, Saari H, Olin M, Kulmala MH. Indoor air aerosol model: transport indoors and deposition of fine and coarse particles. Aerosol Sci Technol 1989;11:11–25.
10. Thornburg J, Ensor D, Rodes C, Lawless P, Sparks L, Mosley R. Penetration of particles in buildings and associated physical factors: part I, model development and computer simulations. Aerosol Sci Technol 2001;34:284–306.
11. Kulmala M, Asmi A, Pirjola L. Indoor air aerosol model: the effect of outdoor air, filtration and ventilation on indoor concentrations. Atmos Environ 1999;33:2133–44.
12. Nazaroff WW, Cass GR. Mathematical modeling of chemically reactive pollutants in indoor air. Environ Sci Technol 1996;20:924–34.
13. Tung TC, Chao CY, Burnett J. A methodology to investigate the particulate penetration coefficient through building shell. Atmos Environ 1999;33:881–93.
14. Christoforou C, Salmon L, Cass G. Passive filtration of airborne particles from buildings ventilated by natural convection: design procedures and case study at the buddist cave temples at Yungang, China. Aerosol Sci Technol 1999; 30:530–44.
15. Schneider T, Kildeso J, Breum N. A two compartment model for determining the contribution of sources, surface deposition and resuspension to air and surface dust concentration levels in occupied rooms. Build Environ 1998;34:583–95.
16. Pirjola L. Effects of the increased UV radiation and biogenic VOC emissions on ultrafine sulphate aerosol formation. J Aerosol Sci 1999;29:355–67.
17. Whitby E, McMurry P, Shankar U, Binkowski F. Modal aerosol dynamics modeling. Research Triangle Park (NC): Atmospheric Research and Exposure Assessment Laboratories, United States Environmental Protection Agency; 1991. Report 600/3–91/020.
18. Raes F, Janssens A. Ion induced aerosol formation in a H_2SO_4-H_2O system—II: numerical calculations and conclusions. J Aerosol Sci 1986;17:715–22.
19. Maroni M, Seifert B, Lindvall T (editors). Indoor air quality—a comprehensive reference book. Amsterdam: Elsevier; 1995. Air quality monographs 3.
20. Hinds WC. Aerosol technology. 2nd ed. New York (NY): John Wiley & Sons; 1998.
21. Corner J, Pendlebury E. The coagulation and deposition of a stirred aerosol. Proc Phys Soc [London] 1951;B64:645–54.
22. Crump JG, Seinfeld JH. Turbulent deposition and gravitational sedimentation of an aerosol in a vessel of arbitrary shape. J Aerosol Sci 1981;12:405–15.
23. Nazaroff WW, Cass GR. Mass-transport aspects of pollutant removal at indoor surfaces. Environ Int 1989;15:367–84.
24. Lai CA, Nazaroff WW. Modelling indoor particle deposition from turbulent flow onto smooth surfaces. J Aerosol Sci 2000;31:463–76.
25. Fuchs N. The mechanics of aerosols. New York (NY): Dover, 1964.
26. Kulmala M, Toivonen A, Mäkelä J, Laaksonen A. Analysis of the growth of nucleation mode particles observed in boreal forest. Tellus 1998;50:449–62.
27. Li W, Hopke PK. Initial size distributions and hygroscopicity of indoor combustion aerosol particles. Aerosol Sci Technol 1993;19:305–16.
28. Li CS, Lin WH, Jenq FT. Characterization of outdoor submicron particles and selected combustion sources of indoor particles. Atmos Environ 1993;27B:413–24.
29. Numerical Algorithms Group. The NAG Fortran library reference, 1991. Mark 15.
30. Holmberg R. Ilmansuodattimien nykyaikaiset suoritusarvot [Current performance values for air filters]. Helsinki: TEKES ja Metalliteollisuuden keskusliitto; 1993. INVENT teknologiaohjelma, technical report 31.
31. Jamriska M, Morawska L, Clark B. Effect of ventilation and filtration on submicrometer particles in an indoor environment. Indoor air 2000;10:19–26.
32. Schneider T, Bohgard M, Gudmunsson A. A semiempirical model for particle deposition onto facial skin and eyes: role of air currents and electric fields. J Aerosol Sci 1994;25:583–93.
33. Weschler CJ, Shields HC. Indoor ozone/terpene reactions as a source of indoor particles. Atmos Environ 1999;33:2301–12.
34. Kulmala M, Pirjola L, Mäkelä JM. Stable sulphate clusters as a source of new atmospheric particles. Nature 2000;404:66–9.